

DreamDrone

Hanyang Kong¹ Dongze Lian¹ Michael Bi Mi² Xinchao Wang¹✉

¹ National University of Singapore ² Huawei International Pte. Ltd.

<https://hyokong.github.io/dreamdrone-page/>



Backyards of Old Houses in Antwerp in the Snow, van Gogh.



the narrow path of a lush oasis in the midst of a vast desert. Palm trees and tropical plants surround a natural spring, creating a haven for wildlife. The golden sands of the desert stretch out in every direction, meeting the clear blue sky at the horizon.

Figure 1. **Visualization results of DreamDrone.** We visualize 30 continuous views for each prompt. The generated scenes are geometry-consistent across adjacent camera views and the details are added gradually when the camera is moving forward.

Abstract

We introduce *DreamDrone*, an innovative method for generating unbounded flythrough scenes from textual prompts. Central to our method is a novel feature-correspondence-guidance diffusion process, which utilizes the strong correspondence of intermediate features in the diffusion model. Leveraging this guidance strategy, we further propose an advanced technique for editing the inter-

mediate latent code, enabling the generation of subsequent novel views with geometric consistency. Extensive experiments reveal that *DreamDrone* significantly surpasses existing methods, delivering highly authentic scene generation with exceptional visual quality. This approach marks a significant step in zero-shot perpetual view generation from textual prompts, enabling the creation of diverse scenes, including natural landscapes like oases and caves, as well as complex urban settings such as *Lego*-style street views. Our code is publicly available.

✉ Corresponding author

1. Introduction

Recent advances in vision and graphics have enabled the synthesis of multi-view consistent 3D scenes along extended camera trajectories, a capability previously explored in works like [3, 7, 17, 19]. This emerging task, termed *perpetual view generation* [19], involves synthesizing views from a flying camera along an arbitrarily long trajectory, starting from a single RGB image. Our study extends this concept, asking: *Can we fly into scenes from any context, real or imagined, using textual prompts?* This paper advances the novel concept of *zero-shot, training-free* perpetual view generation. This entails creating infinite scenes from textual prompts without optimization or fine-tuning on specific datasets. The challenge is considerable: as the camera moves forward, unseen regions must be seamlessly integrated, new details resolved as they approach the camera, all while maintaining photorealism and diversity. Existing research in video synthesis, image inpainting, and view synthesis does not fully address these requirements due to various limitations.

Recent text-to-video generation methods leverage advancements in diffusion models [2, 9, 14, 23, 40, 47] to extend their application to the temporal domain. These approaches show promise, but often require extensive training on large datasets, a costly and resource-intensive endeavor. T2V-0 [14] pioneered zero-shot text-to-video generation, producing notable results. However, limitations are evident as it can generate only a limited number of novel frames, and the quality degrades for longer videos. Additionally, these methods often overlook crucial video elements, such as scene geometry and camera movement. In contrast, text-to-3D methods like [18, 25, 30, 41, 44] utilize geometry to synthesize high-quality novel views but are constrained to limited camera motion and single-object view generation.

SceneScape [7], while conceptually similar to our work, diverges significantly in execution and capability. Its primary strategy involves outfilling regions during backward camera movement using 3D meshes. However, SceneScape encounters challenges with forward-moving cameras and in generating outdoor scenes. These issues stem from 1) difficulty in accurately filling irregular holes and preserving correspondence with original regions, 2) distortions in wrapped images remaining uncorrected, and 3) an inability to adequately detail areas enlarged by forward camera motion. Additionally, its dependence on mesh representations confines SceneScape to indoor scenarios, limiting its versatility. Our comparative analysis in Fig. 4 illustrates these limitations in SceneScape.

In this paper, we introduce *DreamDrone*, a novel method designed to generate infinite scenes from textual prompts. *DreamDrone* leverages off-the-shelf text-to-image diffusion models [34] and depth estimation models [32]. Central to our proposed method is a feature-correspondence-guidance

diffusion process, specifically tailored to create geometry-consistent novel views during the denoising phase. Furthermore, we develop an innovative approach for editing the intermediate latent code, facilitating the generation of subsequent novel views. Complementing this, a cross-view self-attention module is employed to ensure consistent correspondence across adjacent views.

Our experiments demonstrate that the proposed *DreamDrone* effectively leads to high-quality and geometry-consistent scene generation, as evidenced in our results (see Fig. 1 and Figs. 3 and 4 in Sec. 4). Notably, despite other works relying on large-scale data for training, our method exhibits comparable, even superior performance. A significant advantage of *DreamDrone* is its versatility: it is adept not only at generating real-world scenarios but also shows promising capabilities in creating imaginative scenes. In summary, our key contributions are as follows:

- We propose a novel approach for zero-shot text-to-perpetual view generation, capable of producing diverse indoor and outdoor scenes in various imaginative styles. This method achieves significant results without requiring fine-tuning or optimization on specific datasets.
- We develop a novel feature-correspondence-guidance diffusion process to maintain geometric consistency in novel view generation. This approach involves a strategic modification of the diffusion model’s intermediate features, enhancing the fidelity and detail in each newly generated view.
- Extensive experiments demonstrate that *DreamDrone* can generate infinite sequences, exemplified by 30 frames in Fig. 1. It handles a broad spectrum of scenarios, from realistic to fantastical, encompassing oases, caves, and urban scenes in styles like Lego or Van Gogh.

2. Related Works

Perpetual view generation. InfNat [19], InfNat-0 [17], and DiffDreamer [3] use iterative training for long-trajectory perpetual view extrapolation. InfNat [19] pioneered the *perpetual view generation* task with a database for infinite 2D landscapes. InfNat-0 [17] adapted this to 3D, introducing a render-refine-repeat phase for novel views. DiffDreamer [3] improved consistency with image-conditioned diffusion models. However, trained on specific datasets, these methods lack robustness in new scenarios, like urban environments, and their non-text-based conditioning restricts generative capabilities. In very recent concurrent work, SceneScape [7] generates limited scenes when the camera is moving backward, which focuses on 3D-consistent ‘zoom out’ video generation. When the camera is moving forward, there is not any specific mechanism to add details and alleviate distortion. Moreover, SceneScape can only generate limited indoor scenes because they apply a mesh as a unified representation.

Text-to-3D generation. Several text-to-3D generation methods [1, 4, 27, 29, 49] apply text-3D pair databases to learning a mapping function. However, supervised strategies remain challenging due to the lack of large-scale aligned text-3D pairs. CLIP-based [31] 3D generation methods [12, 13, 15, 28, 51] apply pre-trained CLIP model to create 3D objects by formulating the generation as an optimization problem in the image domain. Recent text-to-3D methods like [18, 24, 25, 30, 44] blend text-to-image diffusion models [34] with neural radiance fields [26] for training-free 3D object generation. Other approaches [20, 21, 33, 37] focus on novel view synthesis from a single image, often limited to single objects or small camera motion ranges. Text2room [10] generates 3D indoor scenes from text, but is confined to room meshes. Our *Dream-Drone* diverges by creating endless, diverse indoor and outdoor scenes, in styles ranging from Lego to Van Gogh.

Text-to-video generation. Generating videos from textual descriptions [2, 9, 11, 23, 36, 43, 50] poses significant challenges, primarily due to the scarcity of high-quality, large-scale text-video datasets and the inherent complexity in modeling temporal consistency and coherence. CogVideo [11] addresses this by incorporating temporal attention modules into the pre-trained text-to-image model CogView2 [6]. The video diffusion model [9] employs a space-time factorized U-Net, utilizing combined image and video data for training. Video LDM [2] adopts a latent diffusion approach for generating high-resolution videos. However, these methods typically do not account for the underlying 3D scene geometry in scene-related video generation, nor do they offer explicit control over camera movement. Additionally, their reliance on extensive training with large datasets can be prohibitively costly. While T2V-0 [14] introduced the concept of zero-shot text-to-video generation, its capability is limited to generating a small number of novel frames (up to 8 frames), with diminished quality in longer video sequences.

3. Method

3.1. Preliminaries

In this paper, we implement our method based on the recent state-of-the-art text-to-image diffusion model (*i.e.* Stable Diffusion [34]). Stable diffusion is a latent diffusion model (LDM), which contains an autoencoder $\mathcal{D}(\mathcal{E}(\cdot))$ and a U-Net [35] denoiser. Diffusion models are founded on two complementary random processes. The *DDPM forward* process, in which Gaussian noise is progressively added to the latent code of a clean image: \mathbf{x}_0 :

$$\mathbf{x}_t = \sqrt{\alpha_t}\mathbf{x}_0 + \sqrt{1 - \alpha_t}\mathbf{z}, \quad (1)$$

where $\mathbf{z} \sim \mathcal{N}(0, \mathbf{I})$ and $\{\alpha_t\}$ are the noise schedule.

The *backward* process is aimed at gradually denoising \mathbf{x}_T , where at each step a cleaner image is obtained. This process is achieved by a U-Net ϵ_θ that predicts the added noise \mathbf{z} . Each step of the backward process consists of applying ϵ_θ to the current \mathbf{x}_t , and adding a Gaussian noise perturbation to obtain a cleaner \mathbf{x}_{t-1} .

Classifier-guided DDIM sampling [5] aims to restore images from noise conditioned on the class label. Given the diffusion model ϵ_θ , the latent code \mathbf{x}_t at timestep t , the classifier $p_\theta(y|\mathbf{x}_t)$, and the gradient scale s , the sampling process for obtaining \mathbf{x}_{t-1} is formulated as:

$$\hat{\epsilon} = \epsilon_\theta(\mathbf{x}_t) - \sqrt{\bar{\alpha}_{t-1}}\nabla_{\mathbf{x}_t} \log p_\theta(y|\mathbf{x}_t), \quad (2)$$

and

$$\mathbf{x}_{t-1} = \sqrt{\bar{\alpha}_{t-1}} \cdot \frac{\mathbf{x}_t - \sqrt{1 - \bar{\alpha}_t}\hat{\epsilon}}{\sqrt{\bar{\alpha}_t}} + \sqrt{1 - \bar{\alpha}_{t-1}}\hat{\epsilon}, \quad (3)$$

where α is the denoise schedule.

In the self-attention block of the U-Net, features are projected into queries \mathbf{Q} , keys \mathbf{K} , and values \mathbf{V} . The output of the block \mathbf{o} is obtained by:

$$\mathbf{o} = \mathbf{A}\mathbf{V}, \quad \text{where } \mathbf{A} = \text{Softmax}(\mathbf{Q}\mathbf{K}^\top) \quad (4)$$

The self-attention operation allows for long-range interactions between features.

3.2. Overview

In generating infinite scenes, the process involves two key steps. Firstly, the RGB for the forthcoming frame is calculated based on the RGBD data and camera extrinsics of the current frame. Secondly, to address the presence of black holes in the next frame’s image, inpainting [22, 34, 48] and outpainting [16, 46] techniques are employed for correction. Despite this approach, several challenges arise: 1) The irregular nature of the black holes makes it difficult for existing inpainting methods to fill these areas while maintaining semantic coherence with the rest of the image. 2) Inaccuracies in the depth data can cause distortions in certain image areas when wrapping. These distortions tend to accumulate over time with the movement of the camera, leading to a noticeable decline in image quality. 3) Additionally, as the image advances, it requires the enhancement of details in certain areas, a task at which current inpainting and outpainting methods are inadequate, particularly due to their lack of super-resolution capabilities.

To avoid generating distorted areas, ensure semantic consistency between adjacent frames, and enhance image detail during camera movement, we leverage the robustness and rich semantic capabilities of the denoise phase and decoder in the stable diffusion model. We edit the features of the diffusion based on depth and camera extrinsics, followed by denoising to produce a high-definition image for

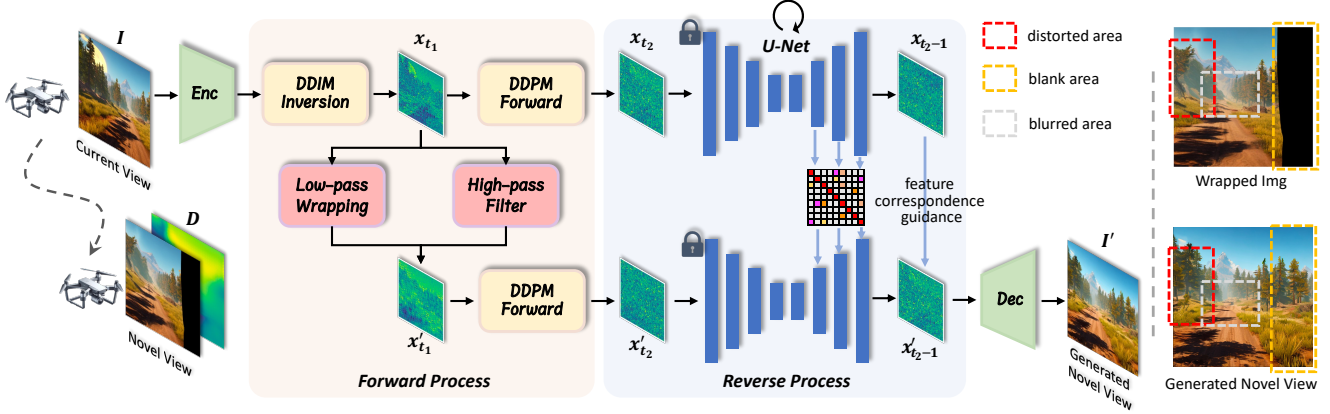


Figure 2. **Overview of DreamDrone.** Starting from a real or generated RGBD (I, D) image at the current view, we apply DDIM backward steps to obtain intermediate latent code x_{t_1} at timestep t_1 using a pre-trained U-Net model. A low-pass wrapping strategy is applied to generate latent code for the next novel view. A few more DDPM forward steps from timestep t_1 to t_2 are followed for enlarging the degree of freedom *w.r.t.* the wrapped latent code. In the reverse progress, we apply pre-trained U-Net to recover the novel view from x'_{t_2} . The cross-view self-attention module and feature-correspondence guidance are applied to maintain consistency between x_{t_2} and x'_{t_2} . The right side shows the wrapped images and our generated novel view I' . Our method greatly alleviates blurring, in-consistency, and distortion. The overall pipeline is zero-shot and training-free.

the subsequent frame. Our comprehensive design is detailed in Fig. 2. Initially, we obtain the latent code of the previous frame’s RGB image at timestep t_1 through the inverse diffusion process. We then wrap the current frame’s latent code using depth information and camera extrinsics. To maintain content and high-frequency detail consistency while wrapping the latent code, we introduce a low-pass wrapping strategy. Then several DDPM (Denoising Diffusion Probabilistic Models) processes are applied to increase the generative process’s flexibility, adding noise from timestep t_1 to t_2 . Finally, we obtain the RGB image of the next frame through the denoising process. For ensuring semantic consistency between adjacent frames, we utilize a cross-frame self-attention strategy, injecting the key and value from the previous frame’s UNet network into the next frame. Furthermore, we propose a feature-correspondence-guidance strategy to influence and maintain semantic consistency between adjacent frames during the denoise latent code process. Our entire pipeline requires only a pre-trained text-to-image diffusion model and a depth estimation model, eliminating the need for any additional training or fine-tuning.

3.3. Wrapping latent codes

The results in the right side of Fig. 2 reveal that directly wrapping images based on camera intrinsics K , extrinsics (R, t) , and depth information leads to regions of distortion in the images. Additionally, the use of inpainting [22, 34, 48] and outpainting [16, 46] models to fill these gaps does not achieve satisfactory outcomes. In pursuit of generating photo-realistic images, and considering the robustness of the denoising process and decoder in the stable

Algorithm 1 Low-pass latent code wrapping

Require: $x_t \triangleright$ latent code at timestep t of current view c

- 1: $F(x_t) \leftarrow FFT(x_t) \triangleright$ Apply Fast Fourier Transform
- 2: Split $F(x_t)$ into F_{low} and F_{high} using threshold σ
- 3: $x_t^{low} \leftarrow IFFT(F_{low}) \triangleright$ Inverse FFT on low-frequency component
- 4: $x_t^{low-wrapped} \leftarrow Wrap(x_t^{low}) \triangleright$ Wrap the low-frequency content
- 5: $F_{wrapped} \leftarrow FFT(x_t^{low-wrapped}) \triangleright$ FFT on wrapped content
- 6: $F' \leftarrow F_{wrapped} + F_{high} \triangleright$ Combine low-frequency of wrapped content with high-frequency of original code
- 7: $x'_t \leftarrow IFFT(F') \triangleright$ Inverse FFT to get latent code for next view c'

return $x'_t \triangleright$ wrapped latent code at timestep t for next view c'

diffusion model, we opt to edit the latent code corresponding to timestep t . PnP [39] and DIFT [38] have shown that the features of diffusion possess strong semantic information, with semantic parts being shared across images at each step. The simplest method for wrapping the latent code follows the same approach as wrapping the image. The only difference between wrapping the latent code and wrapping the image is a slight modification in the camera intrinsics; this entails scaling the camera intrinsics proportionally based on the different resolutions of the image and latent code.

The overall procedure for wrapping the latent code is illustrated in Alg. 1. Initially, a latent code x_t is ob-

tained and transformed via Fast Fourier Transform (FFT) to $F(\mathbf{x}_t)$. This is divided into low-frequency F_{low} and high-frequency F_{high} components, segregated at threshold λ . The key step involves wrapping the Inverse FFT (IFFT) processed low-frequency component $x_t^{\text{low}} = \text{IFFT}(F_{\text{low}})$, forming $x_t^{\text{low-wrapped}}$. Merging $\text{FFT}(x_t^{\text{low-wrapped}})$ with F_{high} , we obtain F_{new} , from which the final latent code $x_t' = \text{IFFT}(F')$ is reconstructed. This approach efficiently preserves high-frequency details, enabling high-fidelity scene generation aligned with text prompts.

3.4. Feature-correspondence-guidance design

After obtaining the latent code x_t' corresponding to the next frame, we employ the DDPM (Denoising Diffusion Probabilistic Models) method to increase the degrees of freedom of the latent code, enabling the generation of richer image details. However, increasing freedom introduces a challenge: the correlation between frames. An unconstrained diffusion denoising process can result in poor semantic correlation between adjacent frames. To address this, we propose a feature-correspondence guidance strategy with a cross-view self-attention mechanism. We introduce these approaches in detail below.

Cross-view self-attention. To maintain consistency between the generated result and the original image, inspired by recent image and video editing works [8, 39, 42, 45], we modify the process of the self-attention module of U-Net when denoising the latent code x_t' . Specifically, we denoise the views for the current and next view together. The key and value of the self-attention modules from the next view are replaced by that of the current view. To be specific, for obtaining the original view, the self-attention module is defined the same as Eq. (4). The modified cross-view self-attention for generating a novel view is defined as:

$$\sigma' = \mathbf{A}'\mathbf{V}, \quad \text{where } \mathbf{A}' = \text{Softmax}(\mathbf{Q}'\mathbf{K}^\top), \quad (5)$$

where \mathbf{Q}' , \mathbf{A}' , and σ' are query, attention matrix, and output features for the novel views. \mathbf{K} and \mathbf{V} are injected keys and values obtained from the self-attention module for generating the original view.

Feature-correspondence guidance. Maintaining geometry consistency between adjacent views using the cross-view self-attention mechanism presents challenges, especially in preserving high-frequency details as the camera moves forward. The recent DIFT study [38] highlights the potential of using intermediate features of diffusion models for accurate point-to-point image matching. Additionally, the concept of vanilla classifier guidance [5] steers the diffusion sampling process using pre-trained classifier gradients towards specific class labels. Building on these

ideas, we integrate feature correspondence guidance into the DDIM process to enhance consistency between adjacent views, addressing the challenge of detail preservation in dynamic scenes.

Specifically, we obtain the features of the current and next view at each timestep t of the DDIM process and calculate the cosine distance between the wrapped original features and features from the next novel views:

$$\mathcal{L}_{sim}^t = \frac{1 - \cos[\text{Wrap}(f_t), f_t']}{2}, \quad (6)$$

where f_t and f_t' are diffusion features extracted from pre-trained U-Net ϵ_θ at timestep t and Wrap is the wrapping functions. The lower \mathcal{L}_{sim}^t , the higher the similarity.

We further introduce the similarity score \mathcal{L}_{sim} to the DDIM sampling process, for generating novel views with geometry consistency. The predicted noise $\hat{\epsilon}$ is formulated as:

$$\hat{\epsilon} = \epsilon_\theta(\mathbf{x}_t) - \lambda\sqrt{\alpha_{t-1}}\nabla_{\mathbf{x}_t}\mathcal{L}_{sim}^t, \quad (7)$$

where λ is the constant hyper-parameter and latent code \mathbf{x}_{t-1} is calculated by Eq. (3)

4. Experiments

Implementation details. We take Stable Diffusion [34] with the pre-trained weights from version 2.1 as the basic text-to-image diffusion and MiDas [32] with weights `dpt_beit_large_512`. The overall diffusion timesteps is 1000. We wrap the latent code at timestep $t_1=21$ and add more degrees of noise to timestep $t_2=441$. The threshold σ for low-pass wrapping is 20 and the hyper-parameter λ for feature-correspondence guidance is 300. Due to the page limit, please refer to the supplementary material (*supp.*) for details.

Baselines. We compare against 1) 2 supervised methods for perpetual view generation: *InfNat* [19] and *InfNat-0* [17]. 2) one text-conditioned scene generation: *SceneScape* [7]. 3) 2 supervised methods for text-to-video generation: *CogVideo* [11] and *VideoFusion* [23]. 4) one method for zero-shot text-to-video generation: *T2V-0* [14].

Evaluation Metrics. The perpetual view generation is evaluated both quantitatively and qualitatively. We evaluate CLIP [31] score, which indicates text-scene alignment for quantitative comparisons. *CogVideo* [11], *VideoFusion* [23], *SceneScape* [7], and *T2V-0* [14] are all engaged in text-conditioned generation tasks. We generated 50 scene-related text prompts using GPT-4 and then created videos using each of the three methods. For the *InfNat* [19] and

<https://huggingface.co/stabilityai/stable-diffusion-2-1-base>
<https://github.com/isl-org/MiDaS>
<https://openai.com/gpt-4>

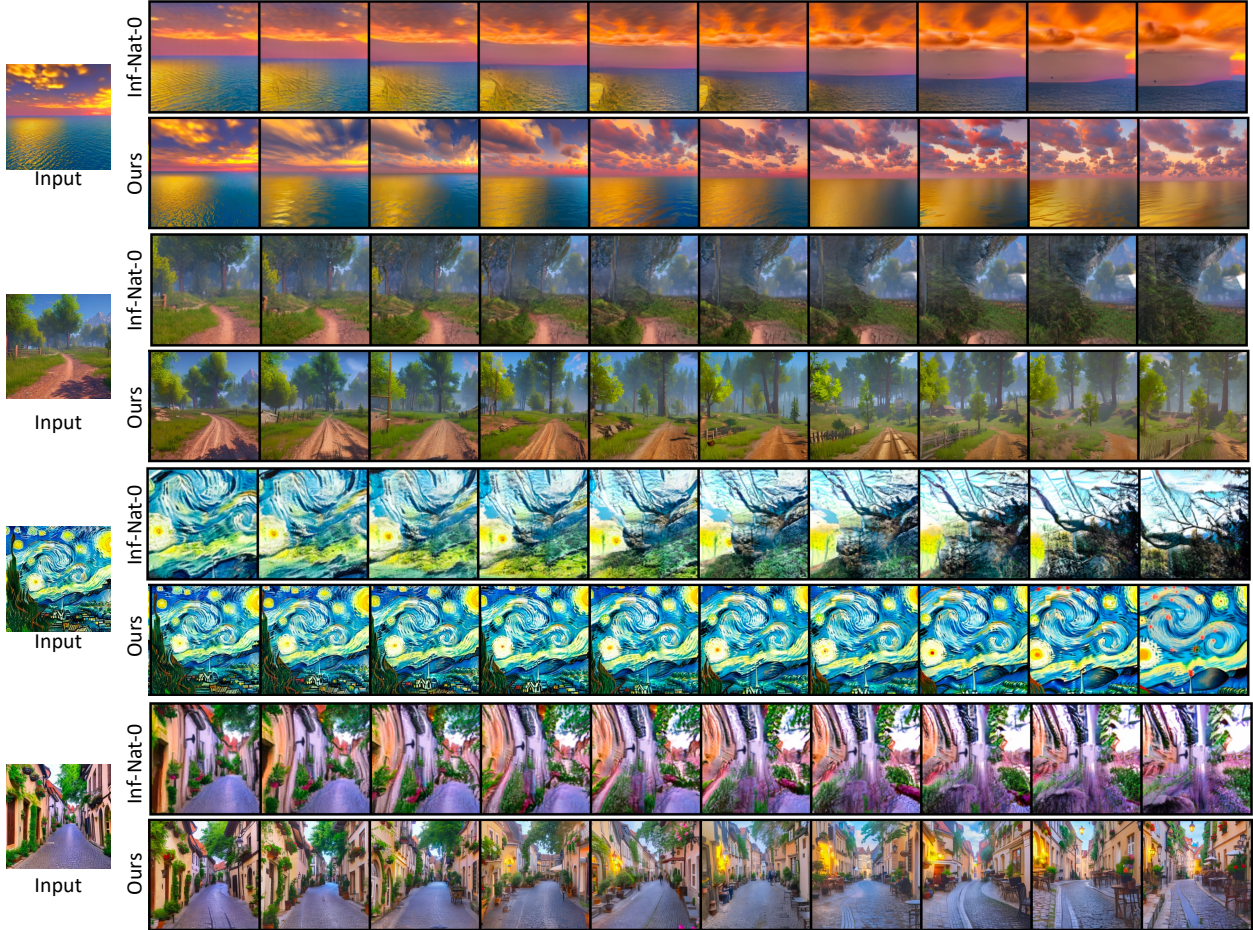


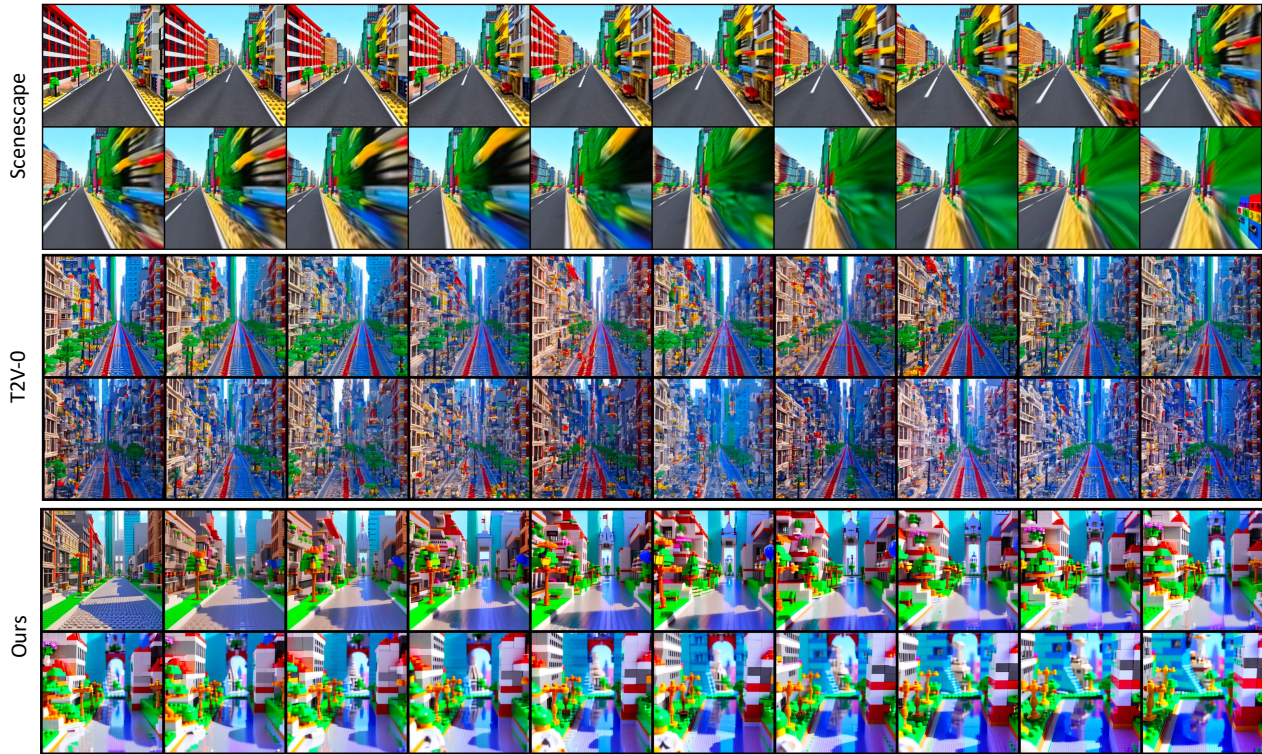
Figure 3. **Qualitative comparisons of InfNat-0 [17] and ours.** We provide four scene images with various styles and categories as start points and ask models to fly through the images. 10 frames are illustrated for each starting point.

InfNat-0 [17] methods, we used Stable Diffusion to generate the initial frame, followed by subsequent frame generation based on this initial frame. We calculated the distance between each generated frame and the text embedding, known as the CLIP score. A high average CLIP score indicates not only that the generated images are more aligned with the corresponding prompts but also that they consistently maintain high quality. Considering that the InfNat [19] and InfNat-0 [17] methods might gradually generate other scenes, we provided 10 very general prompts such as ‘an image of the landscape’ and ‘an image of the mountain’ for these methods, and then selected the highest CLIP score as the CLIP score for the current frame.

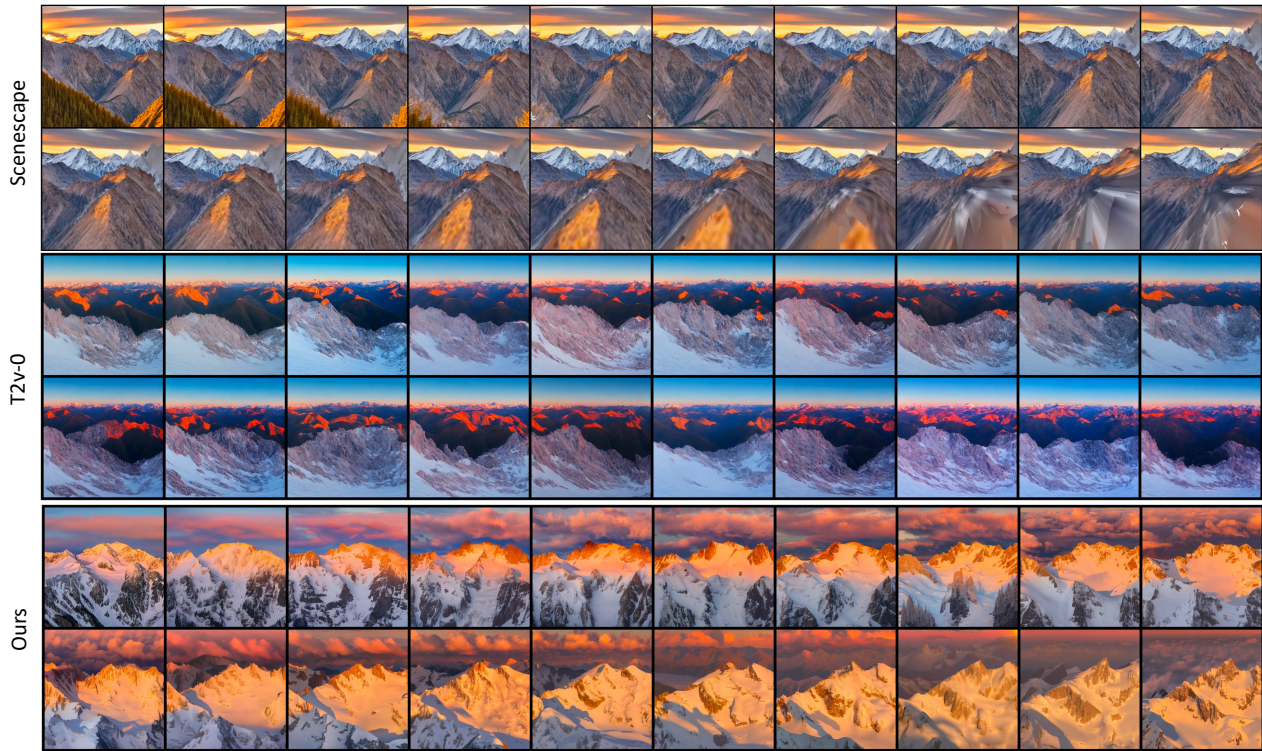
4.1. Quantitative comparison

The quantitative comparison results are shown in Tab. 1. It is evident that the CLIP scores for the InfNat and InfNat-0 methods are low, indicating poor robustness. These methods are not sufficiently versatile to handle infinite scene

generation for any scenario, as also illustrated by the visual results in Fig. 3. CogVideo and VideoFusion, which are supervised text-to-video generation methods, struggle to generate first-person perspective landscapes due to limitations of text-video training datasets. Additionally, their CLIP scores decrease with an increasing number of frames, such as 32 frames, which is corroborated by the visual results in *supp.* T2V-0 [14], SceneScape [7], and our method, both based on the pre-trained stable diffusion model and training-free, have relatively higher CLIP scores. However, as the number of frames increases, SceneScape and T2V-0’s CLIP scores decrease, whereas ours remains constant (please refer to Fig. 4 for qualitative comparisons). We attribute this to our low-pass wrapping strategy, which provides better content guidance for the generated images, and the introduction of feature-correspondence guidance, ensuring the coherence of adjacent frames and thus maintaining a higher CLIP score.



the first view in the city, the street is straight and endless, lego style, 8K.



a panoramic view of a majestic mountain range. The scene should include towering peaks with snow-capped tops, deep valleys, and rugged terrain. The light of the setting sun casts a golden glow on the mountainsides.

Figure 4. **Qualitative comparisons of SceneScape [7], T2V-0 [14], and our DreamDrone.** We visualize 20 continuous frames for each textual prompt. As the camera flies, our method generates geometry-consistent scene sequences.

Table 1. **Quantitative comparison results.** We calculate the average CLIP score [31] across various video lengths.

	8 frames	16 frames	32 frames
InfNat [19]	0.125	0.123	0.118
InfNat-0 [17]	0.128	0.125	0.122
SceneScape [7]	0.263	0.238	0.174
CogVideo [11]	0.255	0.249	0.241
VideoFusion [23]	0.281	0.283	0.272
T2V-0 [14]	0.312	0.305	0.287
Ours	0.320	0.318	0.319

4.2. Qualitative comparison

In our comparison with InfNat-0 [17] (Fig. 3), focusing on various scenes including coastlines, rivers, Van Gogh-style landscapes, and city streetscapes, we identified four main differences: Firstly, InfNat-0 shows proficiency in coastline scenes, a reflection of its training data, but our training-free *DreamDrone* surpasses it in later frames due to InfNat-0’s cumulative errors over time. Secondly, in natural scenes with closer objects, InfNat-0’s flawed generation becomes more apparent, whereas our method maintains consistency. Thirdly, InfNat-0’s limited approach to gap filling leads to poor performance in stylized scenes, in contrast to *DreamDrone* which preserves high-frequency details and frame correspondence. Finally, in urban environments, InfNat-0 struggles significantly, while *DreamDrone* achieves realistic and geometry-consistent views, demonstrating its versatility across varied scenarios.

T2V-0 [14] introduces unsupervised text-conditioned video generation using stable diffusion. SceneScape [7] focuses on ‘zoom out’ effects during backward camera movement. However, as seen in Fig. 4, both methods have limitations. SceneScape struggles with outdoor scenes and forward camera movement, leading to blurred and distorted results after 8 steps due to its reliance on a pre-trained inpainting model. T2V-0 displays a decline in quality beyond the third frame in complex environments like Lego-style cities, likely from its latent code editing approach that compromises frame continuity and geometric consistency. Conversely, our *DreamDrone* excels across various scenes. It maintains detail, continuity, and quality in advancing camera scenarios, evident in even simpler landscapes like mountains where T2V-0 and SceneScape cannot effectively portray dynamic elements like cloud movement. Our approach ensures the preservation of fine details such as shadows and sunlight, creating a more dynamic and realistic video experience. Please refer to *supp.* for more quantitative comparisons.

Our task bears similarities to text-to-video generation, we further provide qualitative comparisons with VideoFusion [23], one of the state-of-the-art methods for text-to-

video generation. Due to the page limit, please refer to *supp.* for detailed comparisons.

4.3. Ablation studies



Figure 5. **Ablation study on the key components of our method.** We perform ablation studies by disabling the key components of our method: feature-correspondence guidance, low-pass wrapping strategy, and cross-view self-attention module.

We perform ablation studies on 1) low-pass feature wrapping, 2) cross-view self-attention module, and 3) feature-correspondence guidance in Fig. 5. Without feature-correspondence guidance and cross-view attention, even if we perform the corresponding wrapping at the feature level, it is challenging to ensure strong consistency between generated adjacent frames (1st row). Direct wrapping of the latent code leads to increasingly blurred images and a loss of high-frequency details. However, the use of our low-pass wrapping strategy effectively ensures that the generated images retain high-definition details (2nd row). Without the guidance of the feature-correspondence guidance mechanism or the presence of a cross-view self-attention module, it is difficult to guarantee the geometric consistency of adjacent frames (3rd and 4th rows). The components in our proposed pipeline enhance each other, ensuring that each generated frame is not only rich in detail but also maintains good consistency with adjacent frames. Please refer to *supp.* for more detailed ablation studies.

5. Conclusion

In this work, we pioneer the concept of zero-shot, training-free text-to-perpetual view generation, introducing *DreamDrone* for generating geometry-consistent scenes. We harness the robust capabilities of a pre-trained text-to-

image diffusion model and develop a novel feature-correspondence-guidance diffusion process for creating novel views. Our quantitative and qualitative analyses underscore *DreamDrone*'s superiority over other state-of-the-art methods. We anticipate that our approach will inspire further innovation in AI-Generated Content (AIGC) and make advanced research accessible to a broader spectrum of researchers.

References

- [1] Miguel Angel Bautista, Pengsheng Guo, Samira Abnar, Walter Talbott, Alexander Toshev, Zhuoyuan Chen, Laurent Dinh, Shuangfei Zhai, Hanlin Goh, Daniel Ulbricht, et al. Gaudi: A neural architect for immersive 3d scene generation. *Advances in Neural Information Processing Systems*, 35:25102–25116, 2022. [3](#)
- [2] Andreas Blattmann, Robin Rombach, Huan Ling, Tim Dockhorn, Seung Wook Kim, Sanja Fidler, and Karsten Kreis. Align your latents: High-resolution video synthesis with latent diffusion models. In *Proceedings of the IEEE/CVF Conference on Computer Vision and Pattern Recognition*, pages 22563–22575, 2023. [2, 3](#)
- [3] Shengqu Cai, Eric Ryan Chan, Songyou Peng, Mohamad Shahbazi, Anton Obukhov, Luc Van Gool, and Gordon Wetzstein. Diffdreamer: Towards consistent unsupervised single-view scene extrapolation with conditional diffusion models. In *Proceedings of the IEEE/CVF International Conference on Computer Vision*, pages 2139–2150, 2023. [2](#)
- [4] Kevin Chen, Christopher B Choy, Manolis Savva, Angel X Chang, Thomas Funkhouser, and Silvio Savarese. Text2shape: Generating shapes from natural language by learning joint embeddings. In *Computer Vision—ACCV 2018: 14th Asian Conference on Computer Vision, Perth, Australia, December 2–6, 2018, Revised Selected Papers, Part III 14*, pages 100–116. Springer, 2019. [3](#)
- [5] Prafulla Dhariwal and Alexander Nichol. Diffusion models beat gans on image synthesis. *Advances in neural information processing systems*, 34:8780–8794, 2021. [3, 5](#)
- [6] Ming Ding, Wendi Zheng, Wenyi Hong, and Jie Tang. Cogview2: Faster and better text-to-image generation via hierarchical transformers. *Advances in Neural Information Processing Systems*, 35:16890–16902, 2022. [3](#)
- [7] Rafail Fridman, Amit Abecasis, Yoni Kasten, and Tali Dekel. Scenescape: Text-driven consistent scene generation. *arXiv preprint arXiv:2302.01133*, 2023. [2, 5, 6, 7, 8](#)
- [8] Michal Geyer, Omer Bar-Tal, Shai Bagon, and Tali Dekel. Tokenflow: Consistent diffusion features for consistent video editing. *arXiv preprint arXiv:2307.10373*, 2023. [5](#)
- [9] Jonathan Ho, Tim Salimans, Alexey Gritsenko, William Chan, Mohammad Norouzi, and David J Fleet. Video diffusion models. *arXiv:2204.03458*, 2022. [2, 3](#)
- [10] Lukas Höllein, Ang Cao, Andrew Owens, Justin Johnson, and Matthias Nießner. Text2room: Extracting textured 3d meshes from 2d text-to-image models. *arXiv preprint arXiv:2303.11989*, 2023. [3](#)
- [11] Wenyi Hong, Ming Ding, Wendi Zheng, Xinghan Liu, and Jie Tang. Cogvideo: Large-scale pretraining for text-to-video generation via transformers. *arXiv preprint arXiv:2205.15868*, 2022. [3, 5, 8](#)
- [12] Ajay Jain, Ben Mildenhall, Jonathan T Barron, Pieter Abbeel, and Ben Poole. Zero-shot text-guided object generation with dream fields. In *Proceedings of the IEEE/CVF Conference on Computer Vision and Pattern Recognition*, pages 867–876, 2022. [3](#)
- [13] Zutao Jiang, Guansong Lu, Xiaodan Liang, Jihua Zhu, Wei Zhang, Xiaojun Chang, and Hang Xu. 3d-togo: Towards text-guided cross-category 3d object generation. In *Proceedings of the AAAI Conference on Artificial Intelligence*, pages 1051–1059, 2023. [3](#)
- [14] Levon Khachatryan, Andranik Movsisyan, Vahram Tadevosyan, Roberto Henschel, Zhangyang Wang, Shant Navasardyan, and Humphrey Shi. Text2video-zero: Text-to-image diffusion models are zero-shot video generators. *arXiv preprint arXiv:2303.13439*, 2023. [2, 3, 5, 6, 7, 8](#)
- [15] Han-Hung Lee and Angel X Chang. Understanding pure clip guidance for voxel grid nerf models. *arXiv preprint arXiv:2209.15172*, 2022. [3](#)
- [16] Jialu Li and Mohit Bansal. Panogen: Text-conditioned panoramic environment generation for vision-and-language navigation. *arXiv preprint arXiv:2305.19195*, 2023. [3, 4](#)
- [17] Zhengqi Li, Qianqian Wang, Noah Snavely, and Angjoo Kanazawa. Infinitemature-zero: Learning perpetual view generation of natural scenes from single images. In *European Conference on Computer Vision*, pages 515–534. Springer, 2022. [2, 5, 6, 8](#)
- [18] Chen-Hsuan Lin, Jun Gao, Luming Tang, Towaki Takikawa, Xiaohui Zeng, Xun Huang, Karsten Kreis, Sanja Fidler, Ming-Yu Liu, and Tsung-Yi Lin. Magic3d: High-resolution text-to-3d content creation. In *Proceedings of the IEEE/CVF Conference on Computer Vision and Pattern Recognition*, pages 300–309, 2023. [2, 3](#)
- [19] Andrew Liu, Richard Tucker, Varun Jampani, Ameesh Makadia, Noah Snavely, and Angjoo Kanazawa. Infinite nature: Perpetual view generation of natural scenes from a single image. In *Proceedings of the IEEE/CVF International Conference on Computer Vision*, pages 14458–14467, 2021. [2, 5, 6, 8](#)
- [20] Minghua Liu, Chao Xu, Haiyan Jin, Linghao Chen, Zexiang Xu, Hao Su, et al. One-2-3-45: Any single image to 3d mesh in 45 seconds without per-shape optimization. *arXiv preprint arXiv:2306.16928*, 2023. [3](#)
- [21] Ruoshi Liu, Rundi Wu, Basile Van Hoorick, Pavel Tokmakov, Sergey Zakharov, and Carl Vondrick. Zero-1-to-3: Zero-shot one image to 3d object. In *Proceedings of the IEEE/CVF International Conference on Computer Vision*, pages 9298–9309, 2023. [3](#)
- [22] Andreas Lugmayr, Martin Danelljan, Andres Romero, Fisher Yu, Radu Timofte, and Luc Van Gool. Repaint: Inpainting using denoising diffusion probabilistic models. In *Proceedings of the IEEE/CVF Conference on Computer Vision and Pattern Recognition*, pages 11461–11471, 2022. [3, 4](#)
- [23] Zhengxiong Luo, Dayou Chen, Yingya Zhang, Yan Huang, Liang Wang, Yujun Shen, Deli Zhao, Jingren Zhou, and

- Tieniu Tan. Videofusion: Decomposed diffusion models for high-quality video generation. In *Proceedings of the IEEE/CVF Conference on Computer Vision and Pattern Recognition*, pages 10209–10218, 2023. 2, 3, 5, 8
- [24] Luke Melas-Kyriazi, Iro Laina, Christian Rupprecht, and Andrea Vedaldi. Realfusion: 360deg reconstruction of any object from a single image. In *Proceedings of the IEEE/CVF Conference on Computer Vision and Pattern Recognition*, pages 8446–8455, 2023. 3
- [25] Gal Metzer, Elad Richardson, Or Patashnik, Raja Giryes, and Daniel Cohen-Or. Latent-nerf for shape-guided generation of 3d shapes and textures. In *Proceedings of the IEEE/CVF Conference on Computer Vision and Pattern Recognition*, pages 12663–12673, 2023. 2, 3
- [26] Ben Mildenhall, Pratul P Srinivasan, Matthew Tancik, Jonathan T Barron, Ravi Ramamoorthi, and Ren Ng. Nerf: Representing scenes as neural radiance fields for view synthesis. *Communications of the ACM*, 65(1):99–106, 2021. 3
- [27] Shentong Mo, Enze Xie, Ruihang Chu, Lewei Yao, Lanqing Hong, Matthias Nießner, and Zhenguo Li. Dit-3d: Exploring plain diffusion transformers for 3d shape generation. *arXiv preprint arXiv:2307.01831*, 2023. 3
- [28] Nasir Mohammad Khalid, Tianhao Xie, Eugene Belilovsky, and Tiberiu Popa. Clip-mesh: Generating textured meshes from text using pretrained image-text models. In *SIGGRAPH Asia 2022 conference papers*, pages 1–8, 2022. 3
- [29] Alex Nichol, Heewoo Jun, Prafulla Dhariwal, Pamela Mishkin, and Mark Chen. Point-e: A system for generating 3d point clouds from complex prompts. *arXiv preprint arXiv:2212.08751*, 2022. 3
- [30] Ben Poole, Ajay Jain, Jonathan T Barron, and Ben Mildenhall. Dreamfusion: Text-to-3d using 2d diffusion. *arXiv preprint arXiv:2209.14988*, 2022. 2, 3
- [31] Alec Radford, Jong Wook Kim, Chris Hallacy, Aditya Ramesh, Gabriel Goh, Sandhini Agarwal, Girish Sastry, Amanda Askell, Pamela Mishkin, Jack Clark, et al. Learning transferable visual models from natural language supervision. In *International conference on machine learning*, pages 8748–8763. PMLR, 2021. 3, 5, 8
- [32] René Ranftl, Katrin Lasinger, David Hafner, Konrad Schindler, and Vladlen Koltun. Towards robust monocular depth estimation: Mixing datasets for zero-shot cross-dataset transfer. *IEEE transactions on pattern analysis and machine intelligence*, 44(3):1623–1637, 2020. 2, 5, 1
- [33] Chris Rockwell, David F Fouhey, and Justin Johnson. Pixel-synth: Generating a 3d-consistent experience from a single image. In *Proceedings of the IEEE/CVF International Conference on Computer Vision*, pages 14104–14113, 2021. 3
- [34] Robin Rombach, Andreas Blattmann, Dominik Lorenz, Patrick Esser, and Björn Ommer. High-resolution image synthesis with latent diffusion models. In *Proceedings of the IEEE/CVF conference on computer vision and pattern recognition*, pages 10684–10695, 2022. 2, 3, 4, 5, 1
- [35] Olaf Ronneberger, Philipp Fischer, and Thomas Brox. U-net: Convolutional networks for biomedical image segmentation. In *Medical Image Computing and Computer-Assisted Intervention—MICCAI 2015: 18th International Conference, Munich, Germany, October 5-9, 2015, Proceedings, Part III 18*, pages 234–241. Springer, 2015. 3
- [36] Uriel Singer, Adam Polyak, Thomas Hayes, Xi Yin, Jie An, Songyang Zhang, Qiyuan Hu, Harry Yang, Oron Ashual, Oran Gafni, et al. Make-a-video: Text-to-video generation without text-video data. *arXiv preprint arXiv:2209.14792*, 2022. 3
- [37] Junshu Tang, Tengfei Wang, Bo Zhang, Ting Zhang, Ran Yi, Lizhuang Ma, and Dong Chen. Make-it-3d: High-fidelity 3d creation from a single image with diffusion prior. *arXiv preprint arXiv:2303.14184*, 2023. 3
- [38] Luming Tang, Menglin Jia, Qianqian Wang, Cheng Perng Phoo, and Bharath Hariharan. Emergent correspondence from image diffusion. *arXiv preprint arXiv:2306.03881*, 2023. 4, 5
- [39] Narek Tumanyan, Michal Geyer, Shai Bagon, and Tali Dekel. Plug-and-play diffusion features for text-driven image-to-image translation. In *Proceedings of the IEEE/CVF Conference on Computer Vision and Pattern Recognition*, pages 1921–1930, 2023. 4, 5
- [40] Vikram Voleti, Alexia Jolicœur-Martineau, and Chris Pal. Mcvd-masked conditional video diffusion for prediction, generation, and interpolation. *Advances in Neural Information Processing Systems*, 35:23371–23385, 2022. 2
- [41] Haochen Wang, Xiaodan Du, Jiahao Li, Raymond A Yeh, and Greg Shakhnarovich. Score jacobian chaining: Lifting pretrained 2d diffusion models for 3d generation. In *Proceedings of the IEEE/CVF Conference on Computer Vision and Pattern Recognition*, pages 12619–12629, 2023. 2
- [42] Wen Wang, Kangyang Xie, Zide Liu, Hao Chen, Yue Cao, Xinlong Wang, and Chunhua Shen. Zero-shot video editing using off-the-shelf image diffusion models. *arXiv preprint arXiv:2303.17599*, 2023. 5
- [43] Yaohui Wang, Xinyuan Chen, Xin Ma, Shangchen Zhou, Ziqi Huang, Yi Wang, Ceyuan Yang, Yinan He, Jiashuo Yu, Peiqing Yang, et al. Lavie: High-quality video generation with cascaded latent diffusion models. *arXiv preprint arXiv:2309.15103*, 2023. 3
- [44] Zhengyi Wang, Cheng Lu, Yikai Wang, Fan Bao, Chongxuan Li, Hang Su, and Jun Zhu. Prolificdreamer: High-fidelity and diverse text-to-3d generation with variational score distillation. *arXiv preprint arXiv:2305.16213*, 2023. 2, 3
- [45] Jay Zhangjie Wu, Yixiao Ge, Xintao Wang, Stan Weixian Lei, Yuchao Gu, Yufei Shi, Wynne Hsu, Ying Shan, Xiaohu Qie, and Mike Zheng Shou. Tune-a-video: One-shot tuning of image diffusion models for text-to-video generation. In *Proceedings of the IEEE/CVF International Conference on Computer Vision*, pages 7623–7633, 2023. 5
- [46] Chiao-An Yang, Cheng-Yo Tan, Wan-Cyuan Fan, Cheng-Fu Yang, Meng-Lin Wu, and Yu-Chiang Frank Wang. Scene graph expansion for semantics-guided image outpainting. In *Proceedings of the IEEE/CVF Conference on Computer Vision and Pattern Recognition*, pages 15617–15626, 2022. 3, 4
- [47] Ruihan Yang, Prakhar Srivastava, and Stephan Mandt. Diffusion probabilistic modeling for video generation. *Entropy*, 25(10):1469, 2023. 2

- [48] Tao Yu, Runseng Feng, Ruoyu Feng, Jinming Liu, Xin Jin, Wenjun Zeng, and Zhibo Chen. Inpaint anything: Segment anything meets image inpainting. *arXiv preprint arXiv:2304.06790*, 2023. 3, 4
- [49] Xiaohui Zeng, Arash Vahdat, Francis Williams, Zan Gojcic, Or Litany, Sanja Fidler, and Karsten Kreis. Lion: Latent point diffusion models for 3d shape generation. *arXiv preprint arXiv:2210.06978*, 2022. 3
- [50] David Junhao Zhang, Jay Zhangjie Wu, Jia-Wei Liu, Rui Zhao, Lingmin Ran, Yuchao Gu, Difei Gao, and Mike Zheng Shou. Show-1: Marrying pixel and latent diffusion models for text-to-video generation. *arXiv preprint arXiv:2309.15818*, 2023. 3
- [51] Renrui Zhang, Ziyu Guo, Wei Zhang, Kunchang Li, Xupeng Miao, Bin Cui, Yu Qiao, Peng Gao, and Hongsheng Li. Pointclip: Point cloud understanding by clip. In *Proceedings of the IEEE/CVF Conference on Computer Vision and Pattern Recognition*, pages 8552–8562, 2022. 3

DreamDrone

Supplementary Material

Abstract

In this supplementary material, we provide more comprehensive ablation studies, comparisons of visual results with text-to-video methods, and additional visual results of our method. Finally, we discuss the limitations of this approach.

6. Implementation details

We take Stable Diffusion [34] with the pre-trained weights from version 2.1 as the basic text-to-image diffusion and MiDas [32] with weights `dpt_beit_large_512`. The overall diffusion timesteps is 1000. We wrap the latent code at timestep $t_1=21$ and add more degrees of noise to timestep $t_2=441$. The threshold σ for low-pass wrapping is 20 and the hyper-parameter λ for feature-correspondence guidance is 300. We conducted the experiments on Titan-RTX GPU. The generated speed is roughly 30 seconds per frame.

7. Ablation studies

In this section, we conduct our ablation studies on each proposed module. First, we explore the impact of wrapping the latent code at timestep t_1 in our pipeline on the generation results, with comparative results shown in Fig. 6. According to the principles of diffusion, a smaller timestep means that the corresponding latent code has less noise, thus retaining more complete content and detailed information. When we wrap the latent code at a smaller timestep (for example, $t_1 = 1$ or 21), it is observed that, with the camera’s movement, *DreamDrone* still maintains its complete content information quite well. As the timestep increases, with more noise, the content information gets somewhat disrupted, and wrapping the latent code then does not yield as favorable results. This experiment demonstrates that the latent code corresponding to a smaller timestep possesses richer geometry and content information.

Next, we investigate how editing the latent code in different ways can enhance the generation results. We set various thresholds for the low-pass wrapping module, where a smaller threshold indicates the retention of less low-frequency information and more high-frequency information. The comparative results are detailed in Fig. 7. The first and second rows display the generation results corresponding to smaller thresholds. It can be observed that setting an excessively small threshold retains too much ineffective



Figure 6. Ablation study on the wrapping timestep t_1 .

or noisy high-frequency information, leading to generated images with an unrealistic abundance of high-frequency details. Conversely, setting the threshold too high, or removing the low-pass wrapping module, results in a lack of retained detail and very blurry images.

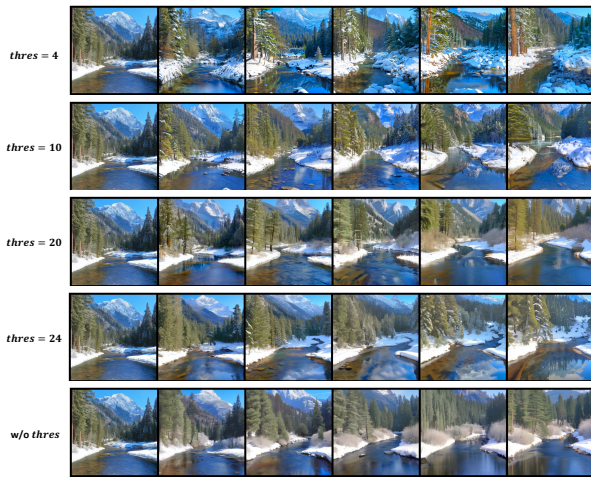


Figure 7. Ablation study on the threshold of the low-pass wrapping module σ .

After obtaining the wrapped latent code, we next investigate the impact of setting t_2 on the generation results. The size of t_2 influences the freedom in the denoising process; a larger t_2 means adding more noise to the wrapped latent code, thereby gaining higher degrees of freedom. The generation results corresponding to different t_2 settings are

<https://huggingface.co/stabilityai/stable-diffusion-2-1-base>
<https://github.com/isl-org/MiDaS>

shown in Fig. 8. A smaller t_2 (for example, $t_2 = 161$ or 241) results in insufficient noise added to the wrapped latent code, leading to increasingly blurred generated images. Setting a larger t_2 produces clearer images with richer details, but an excessively high degree of freedom can decrease the geometric consistency between adjacent frames, adversely affecting their coherence.

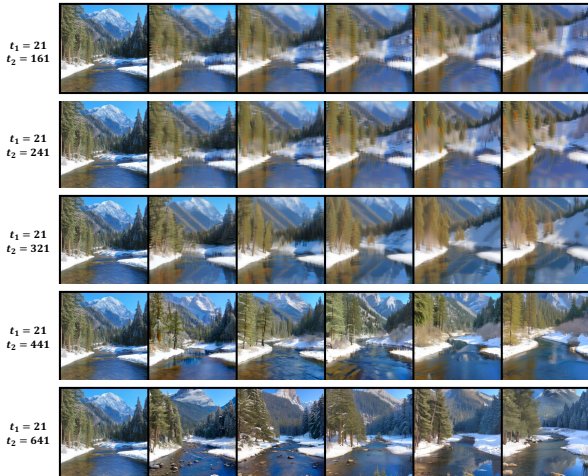


Figure 8. Ablation study on the denoising timestep t_2 .

To ensure geometric consistency between adjacent frames during the denoising process, we introduced a feature-correspondence guidance strategy. Different guidance weights lead to significant variations in generation results, as detailed in Fig. 9. When feature-correspondence guidance is not introduced (*i.e.*, $\lambda = 0$), the generated image sequence maintains content consistency, but some details may not be consistent. The introduction of feature-correspondence guidance ensures the consistency of details between adjacent frames; however, excessively high guidance weights can impact the realism of the generated images.

8. Additional qualitative comparisons

Our task bears similarities to text-to-video generation, with the key difference being that text-to-video generation cannot be controlled by camera pose, and the quality significantly diminishes as the number of generated frames increases. VideoFusion [23], one of the state-of-the-art methods for video generation tasks, has been visually compared with our method, which is illustrated in Fig. 10. It is evident that VideoFusion’s generated results become blurry with an increase in frame count, and the effect of camera movement is less pronounced. In contrast, our method not only generates high-quality continuous scenes but also ensures geometric consistency between frames, clearly conveying the camera’s forward movement. Generating scenes



Figure 9. Ablation study on the weight parameter of feature-correspondence guidance λ .

in constrained environments like caves is more challenging. VideoFusion does not perform well under such prompts, whereas our method effectively demonstrates the effect of the camera advancing forward.

9. More visualization results

In this section, we provide more visualization results. Please refer to Figs. 11 and 12 for details. Moreover, please watch our attached videos for a comprehensive evaluation of our proposed *DreamDrone*.

10. Limitation

Given a prompt, our method can infinitely extend a scene without any training or fine-tuning. However, there are some limitations to our approach. Firstly, as our method is zero-shot and training-free, even with the introduction of feature-correspondence guidance and cross-frame self-attention modules, the correspondence of high-frequency details between adjacent frames is not yet perfect. Secondly, our method heavily relies on the accuracy of depth estimation. Although the stable diffusion model exhibits some robustness, for scenes with special styles, the entirely incorrect depth information leads to unsatisfactory generation results. We plan to address these shortcomings in our future work.

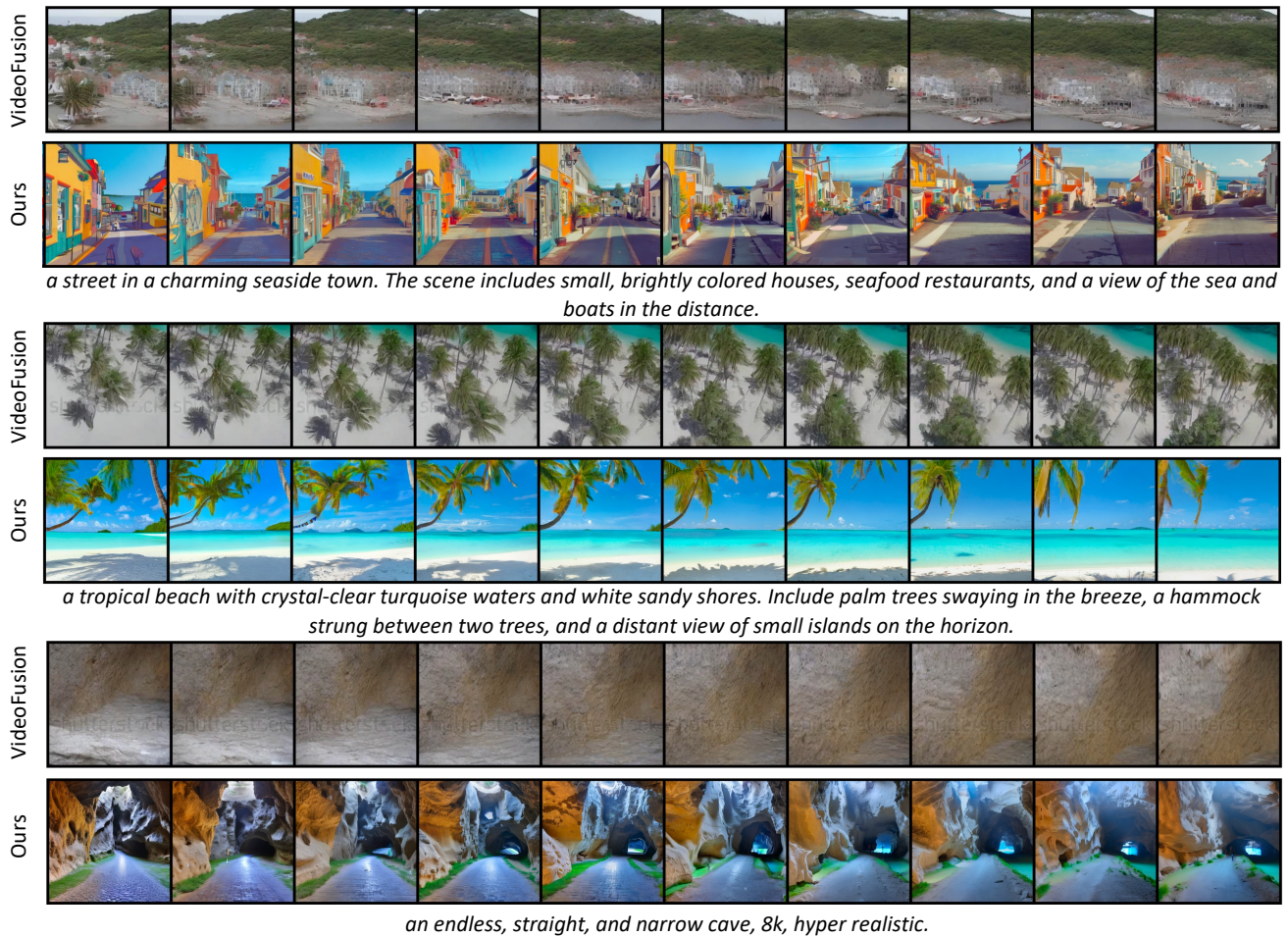
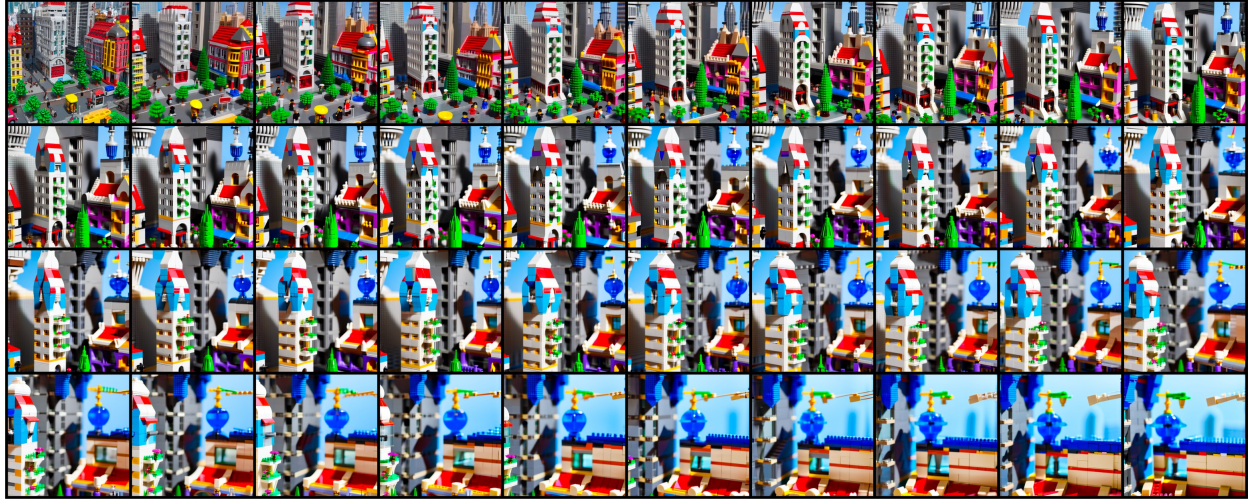


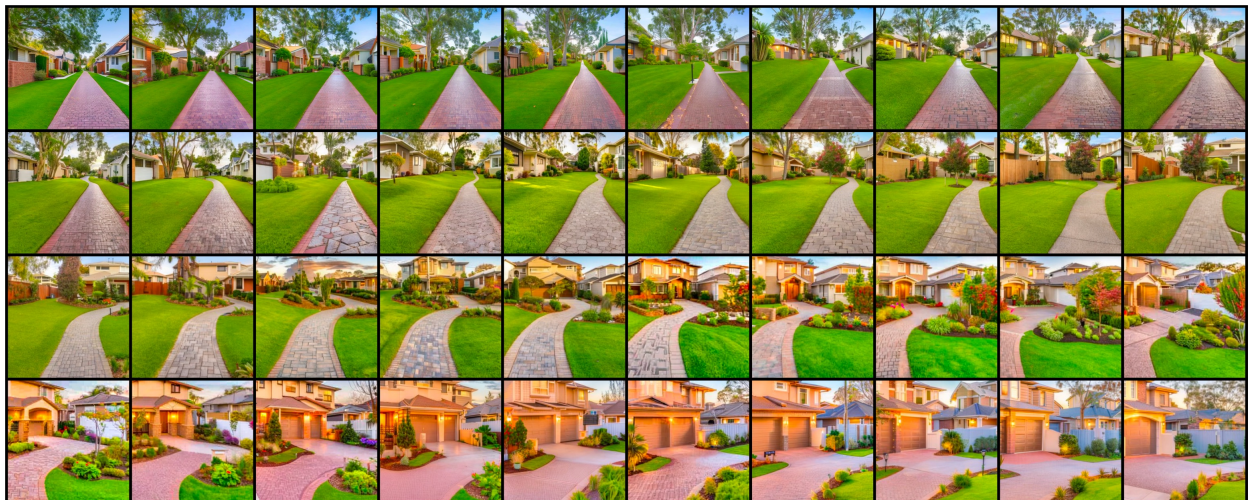
Figure 10. Qualitative comparisons of VideoFusion [23] and our DreamDrone.



aerial view of city, lego style, high-resolution.



a scene of a straight and narrow path meandering through a forest in autumn. The trees are ablaze with red, orange, and yellow leaves, and the ground is covered with fallen foliage. The path leads towards a distant, cozy cottage.



a peaceful narrow and straight suburban street lined with family homes, manicured lawns at each side of the street.

Figure 11. Visualization results of our DreamDrone.



an old cobblestone lane winding through the countryside. The lane passes by traditional stone cottages with thatched roofs and well-tended gardens, evoking a sense of nostalgia and timeless beauty



a scene of an underground tunnel, perhaps part of a mine or an ancient subterranean city. Wooden supports line the walls, and the path is lit by lanterns or torches, casting long shadows and suggesting a journey into the depths.



a surreal path in the style of Salvador Dali. Include melting clocks draped over tree branches and a distant, distorted castle. A pathway of floating stones leads through the scene, giving a sense of surreal progression.

Figure 12. Visualization results of our DreamDrone.